Contract No:

This document was prepared in conjunction with work accomplished under Contract No. 89303321CEM000080 with the U.S. Department of Energy (DOE) Office of Environmental Management (EM).

Disclaimer:

Proceedings of the ASME 2023
Pressure Vessels & Piping Conference
PVP2023
July 16-21, 2023, Atlanta, Georgia, USA

Draft

PVP2023-106906

CMOD COMPLIANCE SOLUTION DETERMINED BY STRESS INTENSITY FACTOR FOR SINGLE EDGE NOTCHED TENSION SPECIMENS IN END-CLAMPED CONDITIONS

Xian-Kui Zhu
Materials Technology
Savannah River National Laboratory
Aiken, SC 29808, USA

ABSTRACT

The oil and gas industry favors to use single edge notched tension (SENT) specimens in the end-clamped conditions to measure less conservative fracture toughness or fracture resistance curves in the low constraint conditions. Usually, the single specimen test approach is adopted to measure J-integral or crack tip opening displacement (CTOD) based resistance curves (simply J-R curves or CTOD-R curves), where the elastic unloading compliance technique is often utilized to monitor the crack growth in the quasi-static conditions, and the instantaneous crack length is inferred from crack mouth opening displacement (CMOD) compliance measured at each loading step during a single specimen test. Several numerical solutions of CMOD compliance were obtained by the finite element analysis for end-clamped SENT specimens. However, these CMOD compliance solutions have varied accuracies and different applicable ranges of crack length ratio a/W. Some of them may be inconsistent with the existing solutions of the stress intensity factor K for the same clamped SENT specimen because the K factor and the CMOD compliance were determined separately in their own FEA calculations. Due to this reason, the present paper develops a more accurate analytical solution of CMOD compliance equation from an accurate full-range K solution for the end-clamped SENT specimens, and thus the proposed analytical solution of CMOD compliance is consistent with the stress intensity factor. Comparisons with different FEA results confirm the higher accuracy of the proposed CMOD compliance solution. Finally, an improved SENT test method is discussed for determining J-R and CTOD-R curves.

KEYWORDS: Fracture toughness, resistance curve, crack length, CMOD compliance, SENT specimen

1. INTRODUCTION

The oil and gas industry has preferred to use the single edge-notched tension (SENT) specimens in the end-clamped conditions to measure less conservative fracture toughness or resistance curves for pipeline steels in the low-constraint conditions. The SENT toughness has been utilized in the strain-based design, fitness for service (FFS) and other fracture mechanics analyses for both offshore and onshore pipelines that contains cracks. Recently, the present author [1] delivered a comprehensive review on fracture toughness test methods and focused on the historical development efforts and current progress for the clamped SENT specimens. Three primary fracture toughness test methods proposed for the end-clamped SENT specimens include the multiple specimen test method developed by Det Norske Veritas (DNV) [2] for a short J-R curve testing, the single specimen test method developed by CANMET [3, 4] for J-R curve and CTOD-R curve testing, and the single specimen method developed by ExxonMobil [5, 6] for CTOD-R curve testing. On this basis, the British Standards Institution (BSI) published the first SENT test standard BS 8571 [7] in 2014 with an update in 2018. In contrast, the American Society for Testing and Materials (ASTM) has not standardized the SENT testing. ASTM developed the most commonly used fracture test standard ASTM E1820 [8] for compact tension (CT) and single-edge notched bend (SENB) specimens, as reviewed by Zhu and Joyce [9].

In an experimental evaluation of J-R curve or CTOD-R curve from a single SENT specimen test, both CANMET and ExxonMobil adopted the elastic unloading compliance method to monitor the incremental crack growth, where their CMOD compliance equations were obtained numerically using the finite element analysis (FEA). These numerical solutions of CMOD compliance have different accuracies and varied applicable ranges of a/W (where a is the crack length and W is the specimen width), and they may be inconsistent with the existing solutions of the stress intensity factor K for the same end-clamped SENT specimen.

To determine a more accurate CMOD compliance solution that is consistent with the K solution, this paper develops a wide-range solution of CMOD compliance equation using a full-range K solution for the clamped SENT specimens. Results verify the higher accuracy of the proposed full-range solution

This work was produced by Battelle Savannah River Alliance, LLC under Contract No. 89303321CEM000080 with the U.S. Department of Energy. Publisher acknowledges the U.S. Government license to provide public access under the DOE Public Access Plan (http://energy.gov/downloads/doe-public-access-plan).

of CMOD compliance in comparison to the existing numerical results for the clamped SENT specimens.

2. BRIEF REVIEW OF COMPLIANCE EQUATIONS FOR CLAMPED SENT SPECIMENS

When the single specimen test approach is utilized for measuring fracture resistance curves, incremental crack growth should be monitored during the fracture test. Conveniently, an instantaneous crack length is estimated from the measured elastic compliance, as recommended in ASTM E1820 [8] for SENB specimens. Experiments showed that the unloading compliance technique is an effective approach to monitor crack length for a single SENT specimen test. With CMOD and its compliance measurements, crack extension can be calculated using an adequate elastic compliance equation. Various elastic compliance equations were obtained from the FEA calculations for clamped SENT specimens, including numerical solutions by Shen et al. [4], Cravero and Ruggieri [10], Fonzo et al. [11] and many others [1].

2.1. CANMET Compliance Inverse Equation

From the elastic FEA calculations for the clamped SENT specimens in the plane strain conditions, CANMET [4, 12] obtained the numerical solution of CMOD compliance inverse equation in an 8th-order polynomial function:

$$\frac{a}{W} = 2.072 - 16.411u + 79.600u^2 - 211.670u^3 + 236.857u^4 + 27.371u^5 - 179.740u^6 - 86.280u^7 + 171.764u^8 \quad (1)$$

where $u = 1/(\sqrt{B_{eff}E'C} + 1)$ is the normalized compliance, E is the Young's modulus, E' = E/(1-ν^2), B_{eff} = B-(B-B_N)^2/B is the effective thickness to consider specimen side groove effect in the three-dimensional (3D) conditions, and C = ΔV/ΔP is the measured CMOD compliance at an unloading or reloading step. Equation (1) is valid for 0.05 ≤ a/W ≤ 0.95 and H/W = 10.

Due to significant rotation occurred during the SENT test, a simple rotation correction factor was proposed by CANMET from the FEA calculation [4]. A major difficulty in use of the unloading compliance technique is the prevalence of apparent negative crack growth at initial loading. This is well-known in the SENB or CT testing, and ASTM E1820 [8] provides an approach to correct the negative crack growth. CANMET [3] developed a similar procedure to obtain corrected initial crack length a_{0q} when apparent negative crack growth is encountered.

2.2. USP Compliance Equation

University of Sao Paulo (USP) developed their unloading compliance technique to monitor the crack size for a single SENT specimen test. Using the elastic FEA simulation for the clamped SENT specimens in the plane strain conditions, Cravero and Ruggieri [10] obtained a simple numerical solution of the CMOD compliance inverse equation in a fifth-order polynomial function:

$$\frac{a}{W} = 1.6485 - 9.1005u + 33.025u^2 - 78.467u^3 + 97.344u^4 - 47.227u^5 \quad (2)$$

The above equation is valid for 0.1≤ a/W ≤0.7 and H/W = 10.

Later, Mathias et al. [13] reported another compliance equation with less accuracy [1]. Recently, Souza & Ruggieri [14] obtained a wide-range CMOD compliance equation:

$$\frac{a}{W} = 1.7548 - 10.7686u + 43.1621u^2 - 108.2553u^3 + 139.5816u^4 - 70.3533u^5 \quad (3)$$

This equation is valid for 0.1≤ a/W ≤0.8 and H/W = 10.

2.3. ExxonMobil Used Compliance Equation

In order to determine a CTOD-R curve, ExxonMobil [6] utilized a double clip gage approach to measure CTOD and the unloading compliance technique to monitor crack growth. They adopted the following CMOD compliance reverse equation in a fifth-order polynomial function:

$$\frac{a}{W} = 1.6446 - 8.7084u + 30.3134u^2 - 69.6092u^3 + 83.5233u^4 - 39.1120u^5 \quad (4)$$

where $u = 1/(\sqrt{B_{eff}EC} + 1)$ is the normalized compliance, and C = ΔV/ΔP is a measured CMOD compliance. Note that the elastic compliance equation (4) was obtained originally by Fonzo et al. [11] and is valid for 0.1≤ a/W ≤0.7 and H/W =10. Specimen rotation effect on the measured compliance was not considered, but an adjustment procedure was proposed by ExxonMobil [6] to correct the apparent negative crack growth at the initial loading for obtaining the physical initial crack length.

2.4. Comparison of Existing Compliance Equations

Figure 1 compares typical CMOD compliance equations obtained by Shen et al. [4] (i.e., CANMET-Eq. (11) as marked in the figure), Cravero and Ruggieri [10] (i.e., USP-Eq. (19)) and Mathias et al. [13] (i.e., USP-Eq. (20)), and ExxonMobil [6] for SENT specimens with H/W=10. In addition, results of the CMOD compliance equations by Tyson et al. [15] and John and Rigling [16] are included in this figure.

It is noted that Fig. 1 was taken from Zhu [1], and thus the equation number marked in the legend of Fig. 1 was used by Reference [1], but not directly used in this paper. In order to examine the accuracy of the numerical solution of CMOD compliance equations, three groups of the plane strain FEA results obtained by Tyson et al. [15] are also included in this figure. Note that Reference [15] indicated that the FEA compliance results of E'BC_{cmod} obtained in the plane strain conditions are equal to the FEA results of EBC_{cmod} obtained in the plane stress conditions. From Fig. 1, the comparison reveals that:

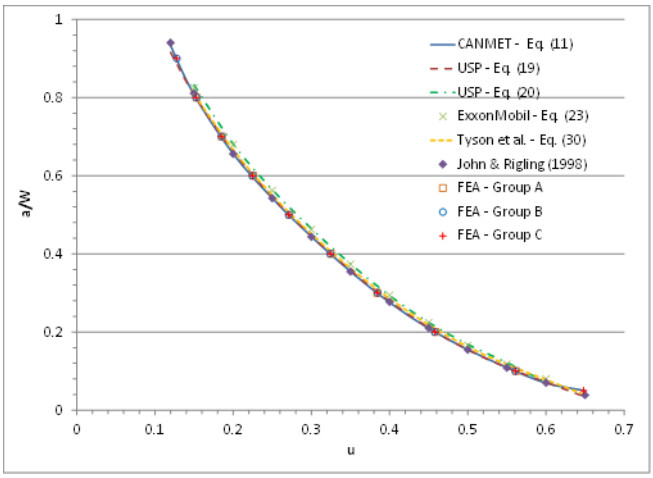

Figure 1. Comparison of available CMOD compliance equations for clamped SENT specimens (taken from [1])

(1) The three sets of FEA results agree very well with each other and with the CANMET solution in Eq. (1), the USP solution in Eq. (2) and the results by John and Rigling [16].

(2) Mathias updated compliance solution [13] is close to ExxonMobil used equation (4), and both are not sufficiently accurate because they deviate from the FEA data.

(3) Tyson's new solution of the CMOD compliance equation [15] also deviates from the FEA data, but less severe in comparison the two results in Item (2).

Further comparisons were provided by Zhu [1] showed that the CANMET solution in Eq. (1) and the USP solution in Eq. (2) are very accurate in comparison to the FEA results obtain by Tyson et al. [15]. Particularly, Equation (1) has an accuracy of -0.36% over 0.05≤ a/W ≤0.9, and Eq. (2) has an accuracy of 0.26% over 0.1≤ a/W ≤0.8. In addition, Souza and Ruggieri [14] showed that the wide range compliance equation (3) has the almost same accuracy as Eq. (2). Therefore, these three CMOD compliance reverse equations are adequate to use in the SENT testing for monitoring crack growth.

3. ANALYTICAL SOLUTION OF CMOD COMPLIANCE

3.1. Crack Compliance Method

For a clamped SENT specimen with an initial crack length of a, based on the crack compliance approach that was developed by Marchand et al. [17], the following relationship between the tensile stress and bending stress is obtained under the condition that the specimen rotation remains zero at the two clamped ends:

$$\frac{\sigma_M}{\sigma_T} = 6\xi_3 \quad \text{and} \quad \xi_3 = \frac{\xi_1}{\xi_2 + 12H/W} \tag{5}$$

where ξ_1 and ξ_2 are two crack compliance functions and expressed in the form of integrals:

$$\xi_1 = 12\pi \int_0^{a/W} \frac{a}{W} f_1\left(\frac{a}{W}\right) f_2\left(\frac{a}{W}\right) d\left(\frac{a}{W}\right) \tag{6}$$

$$\xi_2 = 72\pi \int_0^{a/W} \frac{a}{W} \left[f_2\left(\frac{a}{W}\right) \right]^2 d\left(\frac{a}{W}\right) \tag{7}$$

In the two integrals above, $f_1(a/W)$ and $f_2(a/W)$ are the geometry functions of the K_T factor for a single edge notched (SEN) specimen in pure tension and the K_M factor for a SEN specimen in pure bending, and defined as:

$$f_1\left(\frac{a}{W}\right) = \frac{K_T}{\sigma_T \sqrt{\pi a}} \quad \text{and} \quad f_2\left(\frac{a}{W}\right) = \frac{K_M}{(-\sigma_M)\sqrt{\pi a}} \tag{8}$$

It is noted that an applied bending stress tending to open the crack defines a positive K_M. The bending stress σ_M used in this paper is positive when it tends to close the crack, and thus a negative sign (i.e. $-\sigma_M$) is used in the second of Eq. (8).

Jones [18] reported two very accurate K solutions that are valid over the full range of crack sizes for both pure tension and pure bending. These two K solutions are expressed in the conditions of pure tension and pure bending, respectively, as:

$$f_1(\alpha) = \frac{1}{(1-\alpha)^{3/2}} \left(\begin{array}{c} 1.1212 - 1.6316\alpha + 7.2885\alpha^2 - \\ 18.6443\alpha^3 + 31.7439\alpha^4 - 32.7758\alpha^5 \\ +18.8073\alpha^6 - 4.5179\alpha^7 \end{array} \right) \tag{9}$$

$$f_2(\alpha) = \frac{1}{(1-\alpha)^{3/2}} \left(\begin{array}{c} 1.1211 - 2.9865\alpha + 9.0474\alpha^2 - \\ 22.565\alpha^3 + 38.1996\alpha^4 - 39.5827\alpha^5 \\ +22.4834\alpha^6 - 5.3429\alpha^7 \end{array} \right) \tag{10}$$

where α = a/W. The geometric functions $f_1(\alpha)$ and $f_2(\alpha)$ are continuous over the entire range of crack sizes and have an accuracy of 0.03% and 0.06%, respectively.

To examine accuracy of the K solutions in Eqs. (9) - (10), Figure 2 compares the geometry functions of these K factors obtained by Brown and Srawley [19], Orange [20] and Wilson [21] over the full-range of crack sizes for pure tension and pure bending, with use of two scaled geometrical functions:

$$F_t = (1-a/W)^{3/2} f_1 \quad \text{and} \quad F_b = (1-a/W)^{3/2} f_2.$$

This figure shows that for the pure tension, Brown's solution (valid for a/W ≤ 0.6) and Orange's solution (valid for a/W > 0.6) match well the full-range solutions of Jones [18] with an error of 0.5% and 0.63%, respectively. For the pure bending, Brown's solution (valid for a/W ≤ 0.6) and Wilson's solution (valid for a/W > 0.6) agree with the full-range solutions of Jones [18] with an error of 0.3% and 0.61%, respectively. Thus, Eqs (9) and (10) are very accurate.

Based on the elastic superposition principle, the stress intensity factor K for a clamped SENT specimen is the superposition of the K_T factor for the pure tension and the K_M factor for the pure bending: $K = K_T + K_M$. From Eqs (5) and (8), one has the total K factor for the clamped SENT as:

$$K = \frac{P}{BW}\sqrt{\pi a}(f_1 - 6\xi_3 f_2) = \frac{P}{(BB_N W)^{1/2}} f\left(\frac{a}{W}\right) \quad (11)$$

where $f(a/W) = \sqrt{\pi a / W}(f_1 - 6\xi_3 f_2)$. Based on the two sets of the f_1 and f_2 solutions, Zhu [22, 23] obtained a corrected stress intensity factor solution for the BS 8571 SENT specimens and a family of the full-range stress intensity factor solution for clamped SENT specimens with different heights.

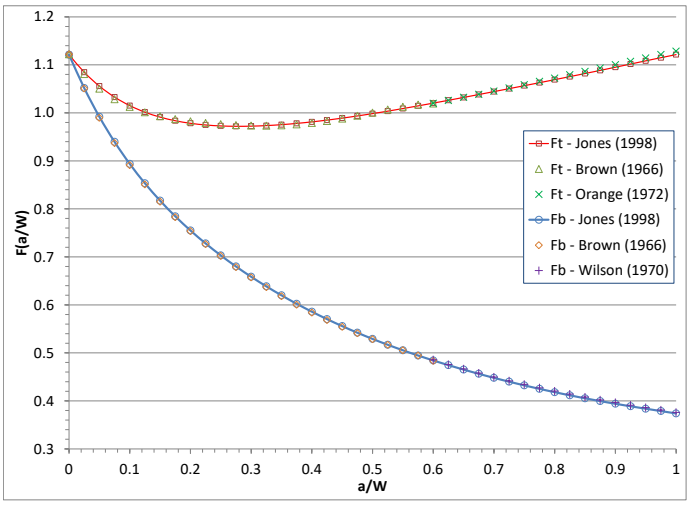

Figure 2. Comparison of scaled geometrical functions of K for pure tension and pure bending

3.2. Relationship between CMOD and Applied Stress

For an infinite center cracked plate (CCP), Westgaard stress function [24] determines a simple relation between the CMOD at the crack center and the remote applied stress for the CCP specimen in the plane stress conditions as CMOD = $4a\sigma_\infty/E$. Tada et al. [25] extended this simple relationship to a finite-cracked CCP specimen in a general form of:

$$CMOD = \frac{4a\sigma_\infty}{E} \mathrm{V(a/w)} \quad (12)$$

where V(a/w) is a dimensionless CMOD geometry function and depends on a/W. Tada et al. [25] provided the CMOD geometry function V(a/W) for the CCP, SENB and pin-loaded SENT specimens. Accordingly, the CMOD for a SEN specimen can be expressed, respectively in pure tension and in pure bending as follows:

$$CMOD_T = \frac{2\sigma_T a}{E} \mathrm{V_T(a/w)} \quad (13)$$

$$CMOD_M = \frac{2\sigma_M a}{E} \mathrm{V_M(a/w)} \quad (14)$$

where V_T and V_M are the CMOD geometry functions and σ_T and σ_M are the remote applied stresses at the specimen ends, respectively for pure tension and pure bending. For an applied load P, the tensile stress $\sigma_T = P/BW$, and for an applied bending moment M, the bending stress $\sigma_M = 6M/BW^2$.

From Eqs (13) and (14), using the superposition principle, the CMOD for a clamped SENT specimen can be expressed as:

$$CMOD = CMOD_T + CMOD_M = \frac{2\sigma_T a}{E}\left[V_T\left(\frac{a}{W}\right) + \frac{\sigma_M}{\sigma_T} V_M\left(\frac{a}{W}\right)\right] \quad (15)$$

Using the bending to tensile stress ratio in Eq. (5), the CMOD for a clamped SENT specimen is written as:

$$CMOD = \frac{2\sigma_T a}{E} V\left(\frac{a}{W}\right) \quad (16)$$

$$V\left(\frac{a}{W}\right) = V_T\left(\frac{a}{W}\right) - 6\xi_3 V_M\left(\frac{a}{W}\right) \quad (17)$$

where ξ_3 is defined in Eq. (5).

Equations (16) and (17) in the analytical displacement approach show that the CMOD can be determined for the clamped SENT specimen if one knows the two K geometry functions and two CMOD geometry functions for the same SEN specimen under loading of pure tension and pure bending. Once CMOD is obtained, the CMOD compliance for the clamped SENT specimen can be simply determined by:

$$EBC_{CMOD} = 2\alpha V(\alpha) = 2\alpha(V_T(\alpha) - 6\xi_3 V_M(\alpha)) \quad (18)$$

3.3. Analytical CMOD and Its Compliance

Tada et al. [25] provided two CMOD geometry functions for the SEN specimen in pure tension and in pure bending:

$$V_T\left(\frac{a}{W}\right) = \frac{2(1.46+3.42(1-\cos(\frac{\pi a}{2W})))}{(\cos(\frac{\pi a}{2W}))^2} \quad (19)$$

$$V_M\left(\frac{a}{W}\right) = 2\left(0.8 - 1.7\frac{a}{W} + 2.4\left(\frac{a}{W}\right)^2 + \frac{0.66}{(1-\frac{a}{W})^2}\right) \quad (20)$$

Those two empirical equations are valid for any a/W with an 1% accuracy. Note that those two CMOD geometry functions were curve-fitted from the results of boundary collocation method (BCM) obtained by Gross et al. [26] with an expected 0.5% accuracy for crack sizes of $0.2 \leq a/W \leq 0.7$.

In addition, Jones [18] reported another two full-range CMOD geometry functions with a higher accuracy for the SEN specimen in pure tension and pure bending. Figure 3 compares these CMOD geometry functions for the SEN specimen in both pure tension and pure bending, where the BCM results by Gross et al. [26] and the FEA results by Bakker [27] are also included for comparison. As evident from this figure, the two CMOD geometry functions given by Tada et al. [25] and Jones [18] agree very well to each other for both loading cases. A smaller difference between the $V_T(a/W)$ for pure tension is observed for crack sizes of $a/W<0.5$ in an error less than 2%.

Moreover, the V_M in Eq. (20) matches well with the FEA data with an error less than 1%. Based on these observations, two CMOD geometry functions in Eqs (19) and (20) are selected in this work for use to determine the CMOD and its compliance for clamped SENT specimens.

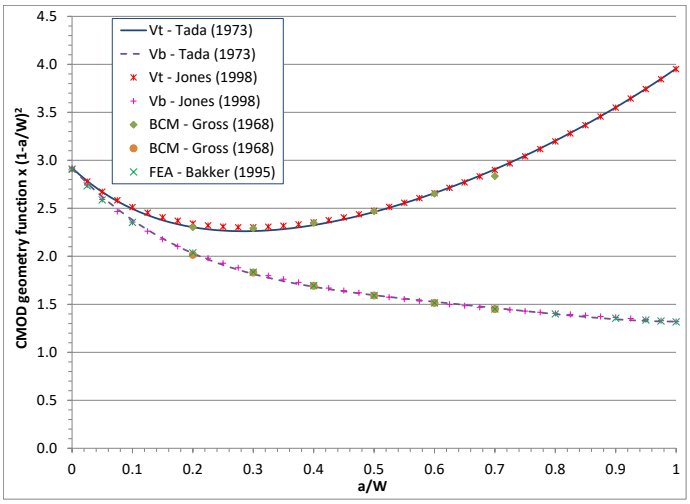

Figure 3. CMOD geometry functions V_T and V_M for the SEN specimen in pure tension and pure bending

Substitution of the two geometry functions of the K factor in Eqs (9) and (10) into the two integrals in Eqs (6) and (7) obtains the two crack compliance functions ξ_1 and ξ_2 through the numerical integration calculation. From Eq. (5) or $\xi_3 = \xi_1/(\xi_2+10H/W)$, one obtains ξ_3 as a function of a/W for a fixed H/W=10. With the ξ_3 results and from Eqs (19) and (20), the CMOD geometry function V(a/W) is determined using Eq. (17) for a clamped SENT specimen. Figure 4 shows the calculated results of the CMOD geometry function for the clamped SENT specimen.

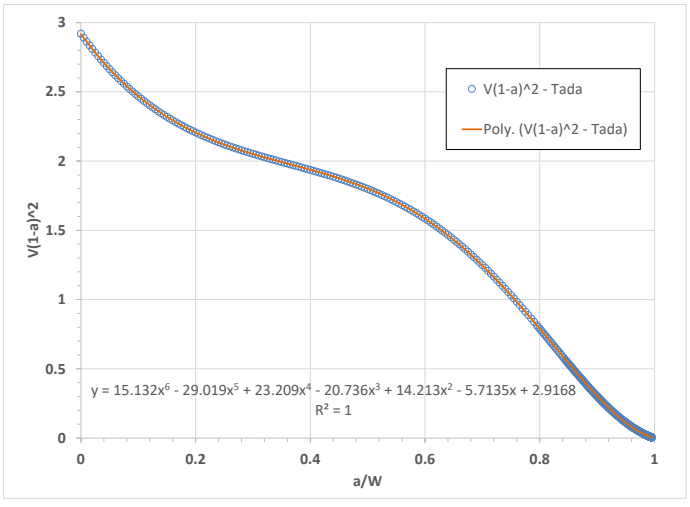

Figure 4. CMOD geometry function and its curve fit function for the clamped SENT specimen with H/W=10

As marked in the above figure, the curve fit function of the CMOD geometry function is expressed as:

$$V(\alpha) = \frac{1}{(1-\alpha)^2}(2.9168 - 5.7135\alpha + 14.213\alpha^2 - 20.736\alpha^3 + 23.209\alpha^4 - 29.019\alpha^5 + 15.132\alpha^6) \quad (21)$$

where α = a/W, and this function is valid over the full range.

Substituting Eq. (21) into Eqs (6) and (8) obtains the full-range analytical CMOD function and the CMOD compliance equation for clamped SENT specimens. In particular, the full-range CMOD equation for H/W = 10 is written as:

$$EBC_{cmod} = \frac{2\alpha}{(1-\alpha)^2}(2.9168 - 5.7135\alpha + 14.213\alpha^2 - 20.736\alpha^3 + 23.209\alpha^4 - 29.019\alpha^5 + 15.132\alpha^6) \quad (22)$$

Figure 5 compares the CMOD compliance solutions proposed in this paper with other available solutions and FEA data for clamped SENT specimens, where the numerical results of CANMAT [4], Cravero and Ruggieri [10], Souza and Ruggieri [14], and Fonzo et al. [11] are calculated using Eqs (1) to (4) , respectively. The FEA data obtained by John and Rigling [16] and Tyson et al. [15] are also included in this figure for comparison. This figure shows that the proposed CMOD compliance equation (22) matches well with the existing numerical solutions and FEA data up to a/W=0.85, and then starts to deviate from the FEA results. This implies that the proposed CMOD compliance equation may overestimate the compliance for very deep cracks of a/W > 0.85. Further FEA data may be needed to verify this implication. On this basis, it is concluded that the proposed CMOD compliance equation (22) is very accurate for crack sizes up to a/W = 0.85. And thus, this CMOD compliance equation (22) is adequate to use for estimating CMOD compliance and crack length if the unloading compliance technique is utilized for a single SENT specimen test in the end-clamped conditions.

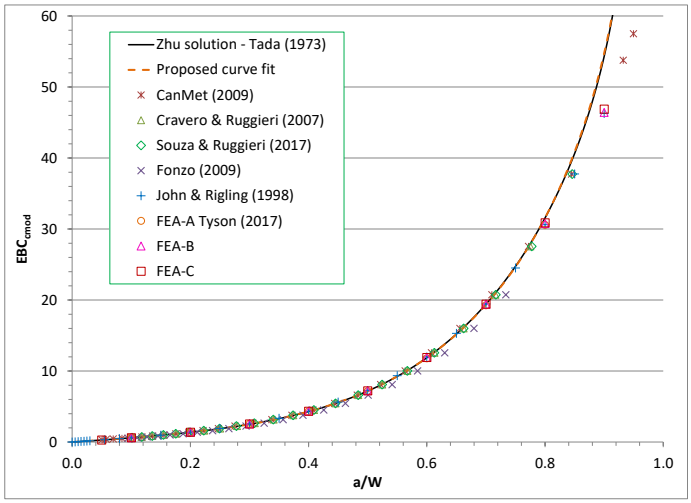

Figure 5. Comparisons of CMOD compliance of proposed solution with other available solutions and FEA data

On the other hand, in the unloading-reloading cycle test of a single SENT specimen, the CMOD elastic compliance can be measured at each loading step for each unloading-reloading cycle. With the measured CMOD compliance data, a compliance reverse equation is needed to calculate the corresponding crack length at the loading step. For this purpose, the data points of the proposed CMOD compliance results up to a/W = 0.9 are employed to determine a curve fit function of the CMOD compliance inverse, as shown in Fig. 6.

Figure 6 show that the curve fit function of the CMOD compliance inverse for H/W = 10 is expressed in a fifth-order polynomial function as:

$$\frac{a}{W} = 1.4747 - 6.3559u + 16.404u^2 - 30.563u^3 + 31.653u^4 - 12.79u^5 \quad (23)$$

where $u = 1/(\sqrt{BEC} + 1)$ is the normalized compliance for the plane stress conditions. The Young's modulus E is replaced using E' = E/(1-ν²) for the plane strain conditions. Figure 6 shows that the CMOD compliance inverse equation (23) is very accurate and valid over the range of 0< a/W <0.9.

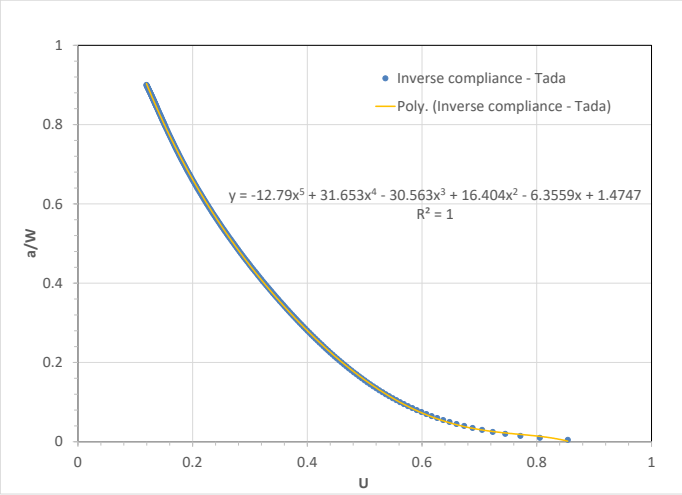

Figure 6. The proposed inverse compliance and its curve fit

Figure 7 compares the CMOD compliance inverse solutions proposed in this paper with other available solutions and FEA data for clamped SENT specimens, where the numerical results of CANMAT [4], Cravero and Ruggieri [10], Souza and Ruggieri [14], and Fonzo et al. [11] are calculated using Eqs (1) to (4) , respectively. The FEA data obtained by John and Rigling [16] and Tyson et al. [15] are also included in Fig. 7 for comparison. The proposed curve fit function of the CMOD compliance reverse equation (23) is added in this figure. Figure 7 shows that the proposed CMOD compliance reverse solution agree very well with those numerical solutions and FEA data in a wide range of crack sizes up to a/W = 0.95.

Based on those comparisons, it is concluded that the CMOD compliance equation (23) is adequate to use for estimating crack length with experimentally measured elastic compliance if the unloading compliance technique is adopted for a single SENT specimen test in the end-clamped conditions.

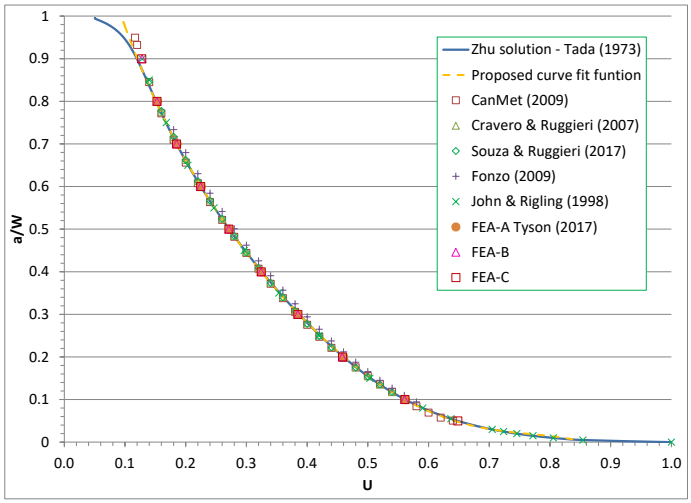

Figure 7. Comparisons of the proposed CMOD compliance reverse solution with numerical solutions and FEA data

4. IMPROVED SENT FRACTURE TEST METHOD

In addition to the CMOD compliance discussed above, this author [28] recently also evaluated all other factors required for determining fracture toughness on an SENT fracture test and proposed an improved SENT fracture test method for determining J-R curves and CTOD-R curves using clamped SENT specimens, as briefly discussed below.

4.1. SENT Test Method for Measuring J-R Curves

Following the guideline of ASTM E1820, the J-integral is separated into an elastic component J_{el} and a plastic component J_{pl}. The elastic J_{el} is determined from the stress intensity factor K using the relationship of $J_{el} = K^2/E'$, and the plastic J_{pl} is calculated from the CMOD-η based equation if the one-point toughness J_{IC} is needed, or from the CMOD-based incremental J-integral equation if a J-R curve is desired to develop using the clamped SENT specimens.

To calculate the J-integral, one needs to use (1) measured applied force P and CMOD data, (2) the K factor solution, (3) CMOD-based geometrical factor η_{CMOD}, (4) load-line displacement (LLD)-based geometrical factor η_{LLD} that is used to calculate the γ factor required for the CMOD-based J-integral equation, and (4) CMOD compliance inverse equation used to estimate crack length during crack growth. Based on the previous studies [28], the best or more accurate solutions of these four quantities are proposed as follows.

1). The K factor solution is the full-range solution that was developed by Zhu [23].

2). The η_{CMOD} and η_{LLD} factor solutions are those obtained by Mathias et al. [13].

3). The CMOD compliance inverse equation is described by Eq. (23) that was developed in this work.

Alternatively, some solutions of the four quantities that have similar accuracy can be used in the calculation of the J-integral. Those include the CANMET K solution [3] or the USP K solution [10], the CANMET η_{CMOD} and η_{LLD} solutions [3], and the CANMET compliance inverse equation (4) or the USP compliance inverse equation (10). Further experimental data for different pipeline steels are needed for assessing the differences in evaluation of J-R curves using those results.

4.2. SENT Test Method for Measuring CTOD-R Curves

As similar to ASTM E1280, it recommends that the J-integral conversion method be used for determining CTOD, where the m factor is the USP solution that was obtained by Sarzosa et al. [13]. If a CTOD-R curve is needed to develop, crack length should be estimated using the CMOD compliance equation (23) that was proposed in this work.

5. CONCLUSIONS

This paper developed a more accurate analytical solution of CMOD and its compliance equation for the end-clamped SENT specimens with H/W=10 by use of the crack compliance approach. From the results, it is concluded that:

(1). The proposed CMOD function and its compliance equation are consistent with the full-range stress intensity factor K solution because they used the same analytical K solutions for the SEN specimens in pure tension and pure bending.

(2). The proposed CMOD function and its compliance equation are valid for the full-range crack sizes and very accurate for crack sizes up to a/W = 0.85, as verified by available FEA results.

(3). The proposed CMOD compliance inverse equation is very accurate over the range of 0< a/W <0.95, as confirmed by the available FEA data and the numerical solutions of the CMOD compliance inverse equations.

As discussed in this paper, further FEA results of the CMOD compliance are needed to verify the proposed CMOD function and the CMOD compliance equation for the clamped SENT specimens. According to the SENT test standard method BS 8571, crack length ratio of SENT specimens of interest is less than 0.5 (or a/W < 0.5). As a result, the proposed more accurate CMOD compliance equation is adequate to be used for estimating more accurate crack length in an unloading compliance test of single SENT specimens in the clamped-end conditions.

ACKNOWLEDGEMENTS

The present author is grateful to the financial support by the Department of Energy (DOE) and its Laboratory Directed Research and Development (LDRD) program through the LDRD Project 2022-00077 at Savannah River National Laboratory.

REFERENCES

[1] Zhu XK. "Progress in Development of Fracture Toughness Test Methods for SENT Specimens," *International Journal of Pressure Vessels and Piping*, Vol. 156, 2017: 40-58.

[2] DNV Recommended Practice DNV-RP-F108, 2006. *Fracture Control for Pipeline Installation Methods Introducing Cyclic Plastic Strain*, Det Norske Veritas, Norway.

[3] Shen G, Gianetto JA and Tyson WR. *Development of Procedure for Low-Constraint Toughness Testing Using a Single-Specimen Technique*, MTL Report No. 2008-18(TR), 2018.

[4] Shen G, Gianetto JA and Tyson WR. "Measurement of J-R Curves using Single-Specimen Technique on Clamped SE(T) Specimens," *Proceedings of 18th International Offshore and Polar Engineering Conference*, Osaka, Japan, June 21-26, 2009.

[5] ExxonMobil Upstream Research Company, *Measurement of Crack-Tip Opening Displacement (CTOD) Fracture Resistance Curves Using Single-Edge Notched Tension (SENT) Specimen*, September 20, 2010.

[6] Tang H, et al. "Development of the SENT Test for Strain-Based Design of Welded Pipelines," *Proceedings of the 8th International Pipeline Conference (IPC2010)*, Calgary, Canada, September 27 - October 1, 2010.

[7] BS 8571-2014, *Method of Test for Determination of Fracture Toughness in Metallic Materials using Single Edge Notched Tension (SENT) Specimens*, British Standards Institution.

[8] ASTM E1820-22, 2022, *Standard Test Method for Measurement of Fracture Toughness*, American Society for Testing and Materials.

[9] Zhu XK and Joyce JA. "Review of Fracture Toughness (G, K, J, CTOD, CTOA) Testing and Standardization," *Engineering Fracture Mechanics*, Vol. 85, 2012: 1-46.

[10] Cravero S and Ruggieri C. "Estimation Procedure of J-Resistance Curves for SE(T) Fracture Specimens Using Unloading Compliance," *Engineering Fracture Mechanics*, Vol. 74, 2007: 2375-2757.

[11] Fonzo A, et al. "Measurement of Fracture Resistance of Pipelines for Strain Based Design," *Proceedings of the 17th PRCI-EPRG-APIA Jointed Technical Meetings on Pipeline Research*, Milan, Italy, May 11-15, 2009.

[12] Shen G, Tyson WR. "Crack Size Evaluation Using Unloading Compliance in Single-Specimen Single-Edge-

Notched Tension Fracture Toughness Testing," *Journal of Testing and Evaluation*, Vol. 37(4), 2009, JTE102368.

[13] Mathias LLS, Sarzosa DFB, Ruggieri C. "Effects of Specimen Geometry and Loading Mode on Crack Growth Resistance Curves of a High-Strength Pipeline Girth Weld," *International Journal of Pressure Vessels and Piping*, Vol. 111-112, 2013: 106-119.

[14] de Souza RF, Ruggieri C. "Revised Wide Range Compliance Solutions for Selected Standard and Nonstandard Fracture Test Specimens based on Crack Mouth Opening Displacement," *Engineering Fracture Mechanics*, Vol. 179, 2017: 77-92.

[15] Tyson WR, Ruggieri C, Zhou W, Wang E. "Effective Modulus for Crack Size Measurement with SE(T) Specimens Using Unloading Compliance," *Journal of Testing and Evaluation*, Vol. 45, 2017, JTE20150488.

[16] John R. and Rigling B. "Effect of Height to Width Ratio on K and CMOD Solutions for a Single Edge Cracked Geometry with Clamped Ends," *Engineering Fracture Mechanics*, Vol. 60, 1998: 147-156.

[17] Marchand N, Parks DM, Pelloux RM. "K_I-Solutions for Single Edge Notch Specimens under Fixed End Displacements," *Engineering Fracture Mechanics,* 38, 1986: 283-294.

[18] Jones IS. "A Wide Range Weight Function for a Single Edge Cracked Geometry with Clamped Ends," *International Journal of Fracture*, Vol. 89, 1998: 1-18.

[19] Brown WF, Srawley JE. *Plane Strain Crack Toughness Testing of High Strength Metallic Materials*, ASTM STP 410, 1966.

[20] Orange TW. "Crack Shapes and Stress Intensity Factors for Edge-Cracked Specimens," *Stress Analysis and Growth of Cracks, Proceedings of the 1971 National Symposium on Fracture Mechanics, Part I, ASTM STP 513*, ASTM, 1972: 71-78.

[21] Wilson WK. "Stress Intensity Factors for Deep Cracks in Bending and Compact Tension Specimens," *Engineering Fracture Mechanics*, Vol. 2, 1970: 169-171.

[22] Zhu XK. "Corrected Stress Intensity Factor Solution for a British Standard Single Edge Notched Tension (SENT) Specimen," *Fatigue & Fracture of Engineering Materials & Structures*, Vol. 39, 2016: 120-131.

[23] Zhu XK. "Full-Range Stress Intensity Factor Solutions for Clamped SENT Specimens," *International Journal of Pressure Vessels and Piping*, Vol. 149, 2017: 1-13.

[24] Westergaard HM. "Bearing Pressures and Cracks," *Journal of Applied Mechanics*, Vol. 6, 1939: 49-53.

[25] Tada H, Paris PC, Irwin GR. 1973, *The Stress Analysis of Cracks Handbook*, Del Research Corporation, Hellertown, PA, USA.

[26] Gross B, Roberts E, Srawley JE. "Elastic displacements for Various Edge Cracked Plate Specimens," *International Journal of Fracture Mechanics*, Vol. 4, 1968: 267-276.

[27] Bakker AD. "Evaluation of Elastic Fracture Mechanics Parameters for Bend Specimens," International Journal of Fracture, Vol. 17, 1995: 323-343.

[28] Zhu XK. "Improved Fracture Toughness Test Method for Single Edge Notched Tension Specimens in Clamped-end Conditions," *Proceedings of the ASME 14th International Pipeline Conference*, September 26-30, 2022, Calgary, Alberta, Canada, IPC2022-86927.